


 Cite this: *RSC Adv.*, 2022, 12, 36138

# Visible-light-driven proton reduction for semi-hydrogenation of alkynes *via* organophotoredox/manganese dual catalysis†

 Xiao-Yu Wang,<sup>‡a</sup> Yong-Qin He,<sup>‡b</sup> Mei Wang,<sup>a</sup> Yi Zhou,<sup>a</sup> Na Li,<sup>b</sup> Xian-Rong Song,<sup>b</sup> Zhao-Zhao Zhou,<sup>b</sup> Wan-Fa Tian<sup>\*a</sup> and Qiang Xiao<sup>\*a</sup>

 Received 12th December 2022  
 Accepted 13th December 2022

DOI: 10.1039/d2ra07920h

[rsc.li/rsc-advances](https://rsc.li/rsc-advances)

Described here is a unprecedented organophotoredox/manganese dual catalyzed proton reduction and its application for semi-reduction of alkynes. The catalytic active pre-catalyst **[Mn-1]** can be feasibly be prepared on gram-scale from  $\text{Mn}(\text{acac})_2 \cdot 2\text{H}_2\text{O}$  in air. This dual catalytic protocol features noble-metal-free catalysts, simple ligand, and mild conditions. Besides, a unique *ortho*-halogen and -hydroxyl effect was observed to achieve high *Z*-stereoselectivity.

Catalytic proton reduction is an effective way to generate metal-hydride (M-H) species, which are key intermediates for  $\text{H}_2$  evolution reactions and hydride transfer reaction.<sup>1</sup> A process of reducing a high valent transition metal to its low-valent state *via* a single electron process, followed by capturing a proton ( $\text{H}^+$ ) to form the key M-H species is always involved in these reactions. The non-precious metals, such as Fe,<sup>2</sup> Co,<sup>3</sup> Ni,<sup>4</sup> and Cu<sup>4b,5</sup> have exhibited extraordinary activity in this field *via* electro- or photocatalytic methodologies. Whereas, Mn, as an analogue of the above metals and the third most abundant transition metal in the Earth's crust, has rarely been reported for proton reduction,<sup>6</sup> and the existing sporadic examples are limited to electrocatalytic  $\text{H}_2$  evolution reactions with structurally complex Mn catalysts.

Recently, photocatalytically generated Co-H has demonstrated its efficiency in catalytic hydride transfer reactions.<sup>1c,7</sup> We thus wondered if Mn-H species can be formed *via* photocatalytic methodologies and be used further for reducing unsaturated bonds. We hypothesize that the reaction might proceed as outlined below (Scheme 1A). The excited photocatalyst PS might be reductively quenched by a sacrificial reagent to afford a reductive photocatalyst  $\text{PS}^{\bullet-}$ , which can reduce high-valent Mn catalysts to low-valent species. The generated Mn species could react with a proton to form Mn-H,

which subsequently undergoes hydrometalation with unsaturated bond followed by protonation to form the hydrogenated product and regenerate high-valent Mn species (Scheme 1A).

Herein, we would like to report the first example of photocatalytically Mn-catalyzed proton reduction for semi-hydrogenation of alkynes by using an **[Mn-1]**/bipyridines catalytic system with DIPEA/AcOH as hydrogen source (Scheme 1B). To the best of our knowledge, such a Mn and photoredox dual catalytic system for reducing unsaturated bonds has not been reported.

Semi-hydrogenation of alkynes to alkenes is a valuable catalytic process,<sup>8</sup> since it leads to configurationally-defined building blocks relevant for the synthesis of pharmaceuticals, agrochemicals, and natural products.<sup>9</sup> Applying the earth-abundant transition metal-based catalysts to realize the reduction is the current research direction.<sup>10</sup> Despite a few Mn catalytic systems have been established by using  $\text{H}_2$ ,  $\text{NH}_3\text{BH}_3$ , or MeOH as hydrogen source, these methods largely rely on sophisticated but complex Mn-pincer complexes.<sup>11</sup> Moreover, these catalytic systems usually require strong base to activate

<sup>a</sup>Key Laboratory of Organic Chemistry of Jiangxi Province, Jiangxi Science & Technology Normal University, Nanchang, 330013, P. R. China. E-mail: tiamwanfa@yeah.net; xiaoqiang@tsinghua.org.cn

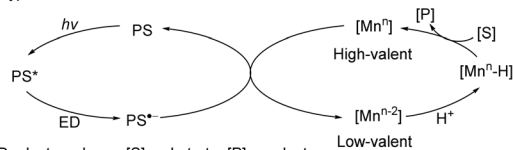
<sup>b</sup>School of Pharmaceutical Science, Nanchang University, Nanchang, 330006, P. R. China

<sup>c</sup>College of Chemistry and Food Science, Nanchang Normal University, Nanchang, P. R. China

† Electronic supplementary information (ESI) available. See DOI: <https://doi.org/10.1039/d2ra07920h>

‡ X.-Y. Wang and Y.-Q. He contributed equally to this work.

A) Our hypothesis: Mn-H formed via  $\text{H}^+$  reduction



B) This work: semi-hydrogenation of alkynes *via* PS/Mn dual catalyzed  $\text{H}^+$  reduction



Scheme 1 Mn-catalyzed reduction *via* photocatalytic protons reduction.



the pre-catalysts accompanied by elevated temperature. Therefore, comparing with the previous work, our protocol is also highlighted by its simple catalyst and mild conditions.

To commend our studies on photocatalytic reduction systems, we selected **1a** as a substrate, DIPEA as a sacrificial reagent, AcOH as an additive, and an organic dye 4CzIPN as a photocatalyst, using blue LED irradiation (Table S2†). Mn(acac)<sub>2</sub>·2H<sub>2</sub>O was chosen as the precatalyst and various *N,N*-bidentate ligands **L1**–**L5** were firstly screened (Table S2,† entry 1). Unfortunately, no reaction occurred. Occasionally, we found that the color of Mn(acac)<sub>2</sub>·2H<sub>2</sub>O gradually changed from yellowish to black under air. Interestingly, this black Mn compound shows partial catalytic activity with **L2** (5,5'-dimethyl-2,2'-bipyridine) as the ligand (not shown). We speculate that Mn(acac)<sub>2</sub>·2H<sub>2</sub>O changed in moist air. Realizing that Mn complexes can undergo rapid transformation in air under alkaline conditions,<sup>12</sup> we conducted a similar reaction using Mn(acac)<sub>2</sub>·2H<sub>2</sub>O as a substrate in the presence of Et<sub>3</sub>N and H<sub>2</sub>O. The mixture rapidly turns to black within 10 minutes, and finally afforded **[Mn-1]** after 2 h stirring (scheme inserted in Fig. 1, see ESI† for detail). A common approach to determine the oxidation of Mn complex is the evaluation of the peak binding energy distance in the multiplet split Mn 3s region in X-ray photoelectron spectra (XPS).<sup>13</sup> Since the 3s peak widths of **[Mn-1]** is 6.2 eV, located at region of Mn<sup>II</sup>, suggesting that **[Mn-1]** still exists mainly in an oxidation of II (Fig. 1, please see the ESI† for details). HRMS analysis demonstrated the full conversion of Mn(acac)<sub>2</sub>·2H<sub>2</sub>O in the reaction that showed in Table 1B (see Fig. S2 and S3†). Furthermore, the UV-vis absorption spectrum of Mn(acac)<sub>2</sub>·2H<sub>2</sub>O, **[Mn-1]**, and Mn oxides (MnO, Mn<sub>2</sub>O<sub>3</sub>, and Mn<sub>3</sub>O<sub>4</sub>) were also collected (Fig. S4†). Among them, Mn oxides displayed no absorption at near infrared region (200–400 nm), but Mn(acac)<sub>2</sub>·2H<sub>2</sub>O and **[Mn-1]** showed strong absorption at 280 nm and 297 nm respectively, which should be attributed to the π–π\* and/or n–π\* electron orbital transitions from acetylacetonate. This observation confirmed that the ligand is still anchored to Mn atom in **[Mn-1]**. Unfortunately, we

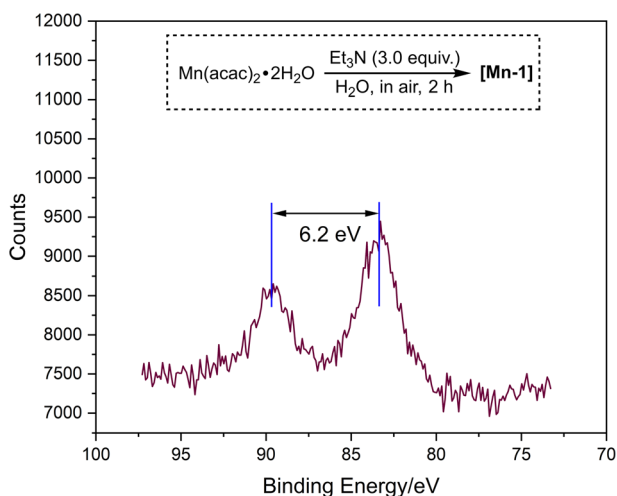
Table 1 Substrate scope<sup>a</sup>

$R^1-C\equiv C-R^2 \xrightarrow[\text{Blue LED (10 W)}]{\begin{array}{l} 4\text{CzIPN (2 mol\%)} \\ \text{[Mn-1] (2.5 mg), L2 (15 mol\%)} \\ \text{DIPEA (3.0 eq.), AcOH (5.0 eq.)} \\ \text{THF (2.0 mL), RT, 6 h} \end{array}} \begin{array}{c} H & H \\   &   \\ R^1-C=C-R^2 \\ 2 \end{array} + \begin{array}{c} H & H \\   &   \\ R^1-C=C-R^2 \\ 3 \end{array}$			
<b>2a</b> : >99% Z:E = 85:15	<b>2b</b> : 95% <sup>[b]</sup> Z:E = 63:37	<b>2c</b> : 99% Z:E = 72:28	<b>2d</b> : 75% Z:E > 95:5
<b>2e</b> : 97% <sup>[c]</sup> Z:E = 79:21	<b>2f</b> : 91% Z:E = 80:20	<b>2g</b> : 74% Z:E = 80:20	<b>2h</b> : 82% Z:E = 76:24
<b>2i</b> : 70% Z:E = 82:18	<b>2j</b> : 78% Z:E = 80:20	<b>2k</b> : 63% <sup>[c]</sup> Z:E = 80:20	<b>2l</b> : 91% Z:E = 75:25
<b>2m</b> : 84% Z:E = 85:15	<b>2n</b> : 0%	<b>2o</b> : 55% <sup>[c]</sup> Z:E > 95:5	<b>2p</b> : 51% <sup>[c]</sup> Z:E > 95:5
<b>2q</b> : 59% <sup>[c]</sup> Z:E > 95:5	<b>2r</b> : 95% Z:E > 95:5	<b>2s</b> : 92% <sup>[c]</sup> Z:E = 60:40	<b>2t</b> : 52% Z:E > 95:5

<sup>a</sup> Conditions: **1** (0.2 mmol), 4CzIPN (2 mol%), **[Mn-1]** (2.5 mg), **L2** (15 mol%), DIPEA (3.0 eq.), and AcOH (5.0 eq.) in THF (2.0 mL) under blue LED (10 W) irradiation. The total isolated yields of Z- and E-alkenes are shown, and the Z/E ratio was determined by <sup>1</sup>H NMR analysis. <sup>b</sup> 24 h. <sup>c</sup> 12 h.

have not been able to determine the exact structure of **[Mn-1]** at this stage.

Nonetheless, this Mn complex is catalytically active. Notably, **[Mn-1]** catalyzes the semi-reduction reaction when employing **L2** as the ligand, giving alkene products with a yield of 64% (entry 3). Further ligand's screening revealed that **L5** could also catalyze the reaction, but inferior yield was obtained (Table S2,† entries, 2, 4–6). Furthermore, the bidentate phosphine ligand dppp failed to promote the reaction (Table S2,† entry 7). Solvent screening revealed that THF gave the full conversion of **1a** to alkenes with a Z/E ratio of 85/15 (Table S2,† entry 8). Other polar solvents such as CH<sub>3</sub>CN and acetone totally inhibited the semi-hydrogenation (Table S2,† entry 9). However, the Mn<sup>III</sup> compound Mn(acac)<sub>3</sub> failed to catalyze the reaction (Table S2,† entry 10). Similarly, changing the additive of AcOH to H<sub>2</sub>O totally suppressed the transformation (Table S2,† entry 11). Photocatalyst screening revealed that Ir[ppy]<sub>2</sub>(dtbbpy)PF<sub>6</sub> catalyzed the reaction with low yield (Table S2,† entries 12 and 13). Control experiments confirmed that the photocatalyst, Mn complex, DIPEA, AcOH, and light are all essential to the reaction (Table S2,† entries 14–17). Additionally, Hg poisoning

Fig. 1 XPS spectra of Mn-3s regions of **[Mn-1]**.

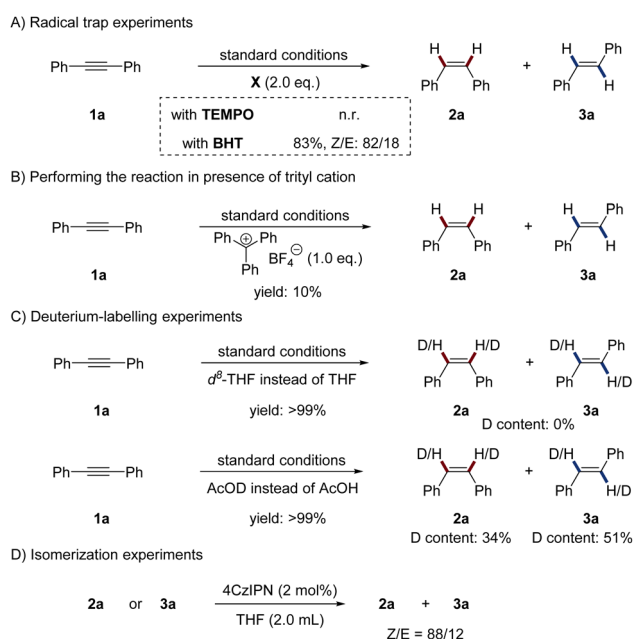
experiments confirmed the homogenous nature of this catalytic system (Table S2,† entry 18). Besides, Mn oxides such as MnO, Mn<sub>2</sub>O<sub>3</sub> and Mn<sub>3</sub>O<sub>4</sub> displayed no activity (Table S2,† entry 19). Of note that none of the over-reduced product **4a** was observed under all conditions tested. Meanwhile, we found that the catalytic active pre-catalyst can also be feasible prepared on gram-scale by just evaporating the solvent in the mixture of Mn(acac)<sub>2</sub>·2H<sub>2</sub>O and H<sub>2</sub>O at 80 °C in air (see ESI† for detail).

With the optimal conditions established, we evaluated the substrate scope of this dual-photoredox Mn catalytic system (Table 1). A range of electronically- and sterically-differentiated internal alkynes were subjected to the conditions. Notably, *para*-substituted alkynes were smoothly semi-hydrogenated to alkenes in good to excellent yields with *Z*-major selectivity (**2a–2l**, 63–99%, *Z*:*E* 63:37→95:5). Reducible groups including chloro, bromo, and ester were tolerated in the reducible conditions. Methoxy at the meta-position did not affect the reaction efficiency, furnishing **2e** and **2m** in 97% and 84% yields, respectively. Interestingly, *ortho*-halogen or hydroxyl substituted diphenylalkynes (**1o–1r**), as well as propargyl alcohol (**1t**) produced the corresponding alkenes with exclusively *Z* selectivity with moderate to excellent yields (**2o–2r**, **2t**, 51–95%, *Z*:*E* >95:5). By sharp comparison, *ortho*-methylated diphenylalkyne **1n** did not proceed under the standard reaction conditions. The coordination effect may contribute to the exclusive *Z*-stereoselectivity.<sup>14</sup> Specifically, stereochemically well-defined (*Z*)-*ortho*-halogen alkenes are important intermediates for diverse functionalization.<sup>15</sup> Moreover, the strongly coordinating heterocycle thiophene (**1s**) was also compatible with the conditions. Terminal alkynes were not compatible under these conditions.

To gain insight into the mechanism of the novel photoredox/manganese dual catalysis, several control experiments were

conducted. To probe a potential radical mechanism, the addition of radical traps to the reaction was investigated (Scheme 2A). When 2 equivalents of 2,2,6,6-tetramethylpiperidine-1-oxyl (TEMPO) were added to the standard reaction, the reaction was completely inhibited. However, 2,6-di-*tert*-butyl-4-methylphenol (BHT) only slightly reduced the reaction yield. Realizing that radical traps might react with the metal-hydride to inhibit the reaction, we thus deduced that radical species might not involve in the catalytic cycle.<sup>16</sup> We surmised that a Mn–H species might be generated in the reaction and be an essential component for product formation. To test this hypothesis, we performed the reaction in the presence of the trityl cation, which is known to be a hydride abstractor for organometallic compounds.<sup>17</sup> As anticipated, the reaction was almost completely inhibited by adding stoichiometric amounts of triphenylcarbenium tetrafluoroborate (Scheme 2B). Deuterium labelling experiments were performed to investigate the H<sub>2</sub> source of the reaction (Scheme 2C). When the reaction was conducted in d<sup>8</sup>-THF, no deuterium was incorporated into the alkenes. Using AcOD instead of AcOH lead to 34% of D-incorporation in **2a** and 51% of D-incorporation in **3a**. Because DIPEA always serves as both an electron donor and a proton donor in reductive photoredox catalysis,<sup>1b,8</sup> we thus deduced that both DIPEA and AcOH work as the H<sub>2</sub> source. Next, isomerization experiments were conducted by employing **2a** or **3a** as substrates without the Mn complex, AcOH and DIPEA (Scheme 2D). The same *Z/E* selectivity as the standard reaction was observed, indicating that photo-induced energy transfer process is the decisive factor for the stereoselectivity.<sup>18</sup>

Additional experiments were performed to probe the reaction pathway. First, the light on-off experiments confirmed the intersection of photoredox with Mn catalysis (Fig. 2A). Second, Stern–Volmer luminescence quenching studies showed that only Mn complex can quench the excited photocatalyst 4CzIPN at a high rate, indicating that efficient electron transfer occurs between excited 4CzIPN and the Mn complex (Fig. 2B). Cyclic voltammetry measurements of the [Mn-1]/L2 complex showed two successive reducible peaks positioned at –1.13 V vs. SCE and –1.43 V vs. SCE (see ESI) corresponding to the respective reductive potential of Mn<sup>II/I</sup> and Mn<sup>I/0</sup>. Since these reductive potentials are less negative than the oxidative potential of the excited photocatalyst 4CzIPN\* ( $E_{1/2 \text{ red}}^{\text{PC}^+/\text{PC}^*} = -1.25 \text{ V vs. SCE}$ )<sup>19</sup> or within its roughly 200 mV range,<sup>20</sup> we thus believe that single electron reduction of Mn complex by the excited photocatalyst is possible.



Scheme 2 Control experiments.

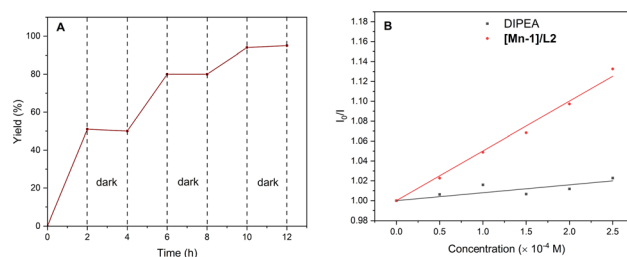


Fig. 2 (A) Light on-off experiments and (B) Stern–Volmer luminescence quenching plot.



Based on above experiments, we supposed that the reaction should involve a photoreduction of high-valent Mn to low-valent state in present of DIPEA, and Mn–H species formation *via* capturing of H<sup>+</sup> by low-valent Mn, although we haven't been able to determine the exact structure of [Mn-1] yet (Scheme S3†).

In conclusion, we report a novel photocatalytic transfer semi-reduction of alkynes through dual Mn and photoredox catalysis. This protocol enables the semi-reduction of a broad range of alkynes with *Z*-major or -exclusive selectivity at room temperature using a simple bipyridine ligand. Although the definitive catalyst structure has not yet been determined, we believe this work will stimulate enthusiasm in the area of Mn-photoredox dual catalysis.

## Conflicts of interest

There are no conflicts to declare.

## Acknowledgements

We gratefully acknowledge the Natural Science Foundation of China (No. 21861016, 22001101), the Science Foundation of Jiangxi Province (No. 20212BAB203009, 20212BAB213014, and 20212BAB213027), and Jiangxi Science & Technology Normal University (No. 2018BSQD024, Doctor Startup Fund) for financial support.

## Notes and references

- (a) W. T. Eckenhoff, *Coord. Chem. Rev.*, 2018, **373**, 295; (b) A. Mazzeo, S. Santalla, C. Gaviglio, F. Doctorovich and J. Pellegrino, *Inorg. Chim. Acta*, 2021, **517**, 119950; (c) M. Kojima and S. Matsunaga, *Trends Chem.*, 2020, **2**, 410.
- (a) F. Gärtner, B. Sundararaju, A.-E. Surkus, A. Boddien, B. Loges, H. Junge, P. H. Dixneuf and M. Beller, *Angew. Chem., Int. Ed.*, 2009, **48**, 9962; (b) A. C. Cavell, C. L. Hartley, D. Liu, C. S. Tribble and W. R. McNamara, *Inorg. Chem.*, 2015, **54**, 3325.
- (a) J. L. Dempsey, B. S. Brunschwig, J. R. Winkler and H. B. Gray, *Acc. Chem. Res.*, 2009, **42**, 1995; (b) J. Willkomm and E. Reisner, *Bulletin of Japan Society of Coordination Chemistry*, 2018, **71**, 18.
- (a) S. Wiese, U. J. Kilgore, D. L. DuBois and R. M. Bullock, *ACS Catal.*, 2012, **2**, 720; (b) X.-S. Hong, D. Huo, W.-J. Jiang, W.-J. Long, J.-D. Leng, L. Tong and Z.-Q. Liu, *Chemelectrochem*, 2020, **7**, 4956.
- A. M. Abudayeh, O. Schott, H. L. C. Feltham, G. S. Hanan and S. Brooker, *Inorg. Chem. Front.*, 2021, **8**, 1015.
- V. Kaim and S. Kaur-Ghumaan, *Eur. J. Inorg. Chem.*, 2019, **2019**, 5041.
- (a) P. Rai, K. Maji and B. Maji, *Org. Lett.*, 2019, **21**, 3755; (b) W. F. Tian, Y. Q. He, X. R. Song, H. X. Ding, J. Ye, W. J. Guo and Q. Xiao, *Adv. Synth. Catal.*, 2020, **362**, 1032; (c) Y.-L. Li, S.-Q. Zhang, J. Chen and J.-B. Xia, *J. Am. Chem. Soc.*, 2021, **143**, 7306.
- (a) A. M. Kluwer and C. J. Elsevier, in *The Handbook of Homogeneous Hydrogenation*, ed. J. G. d. Vries. and C. J. Elsevier, 2006, p. 374; (b) C. Oger, L. Balas, T. Durand and J.-M. Galano, *Chem. Rev.*, 2013, **113**, 1313.
- J. M. J. Williams, in *Preparation of alkenes: a practical approach*, Oxford, U. K., 1996.
- D. Baidilov, D. Hayrapetyan and A. Y. Khalimon, *Tetrahedron*, 2021, **98**, 132435.
- (a) A. Brzozowska, L. M. Azofra, V. Zubar, I. Atodiresei, L. Cavallo, M. Rueping and O. El-Sepelgy, *ACS Catal.*, 2018, **8**, 4103; (b) M. Garbe, S. Budweg, V. Papa, Z. Wei, H. Hornke, S. Bachmann, M. Scalone, A. Spannenberg, H. Jiao, K. Junge and M. Beller, *Catal. Sci. Technol.*, 2020, **10**, 3994; (c) J. Sklyaruk, V. Zubar, J. C. Borghs and M. Rueping, *Org. Lett.*, 2020, **22**, 6067; (d) V. Zubar, J. Sklyaruk, A. Brzozowska and M. Rueping, *Org. Lett.*, 2020, **22**, 5423; (e) R. A. Farrar-Tobar, S. Weber, Z. Csendes, A. Ammaturo, S. Fleissner, H. Hoffmann, L. F. Veiros and K. Kirchner, *ACS Catal.*, 2022, **12**, 2253; (f) A. Torres-Calis and J. J. Garcia, *Catal. Sci. Technol.*, 2022, **12**, 3004.
- (a) J. J. Morgan, *Geochim. Cosmochim. Acta*, 2005, **69**, 35; (b) M. Sankaralingam, Y.-M. Lee, S. H. Jeon, M. S. Seo, K.-B. Cho and W. Nam, *Chem. Commun.*, 2018, **54**, 1209.
- (a) J. W. Murray, J. G. Dillard, R. Giovanoli, H. Moers and W. Stumm, *Geochim. Cosmochim. Acta*, 1985, **49**, 463; (b) J. L. Junta and M. F. Hochella, *Geochim. Cosmochim. Acta*, 1994, **58**, 4985.
- J. Chen, C. Chen, C. Ji and Z. Lu, *Org. Lett.*, 2016, **18**, 1594.
- (a) Z. Li and R. J. Twieg, *Chem.–Eur. J.*, 2015, **21**, 15534; (b) T. Matsushima, S. Kobayashi and S. Watanabe, *J. Org. Chem.*, 2016, **81**, 7799.
- (a) A. C. Albéniz, P. Espinet, R. López-Fernández and A. Sen, *J. Am. Chem. Soc.*, 2002, **124**, 11278; (b) J. R. Carney, B. R. Dillon, L. Campbell and S. P. Thomas, *Angew. Chem., Int. Ed.*, 2018, **57**, 10620.
- (a) D. A. Straus, C. Zhang and T. D. Tilley, *J. Organomet. Chem.*, 1989, **369**, C13; (b) S. R. Bahr and P. Boudjouk, *J. Org. Chem.*, 1992, **57**, 5545.
- (a) K. Singh, S. J. Staig and J. D. Weaver, *J. Am. Chem. Soc.*, 2014, **136**, 5275; (b) W. Cai, H. Fan, D. Ding, Y. Zhang and W. Wang, *Chem. Commun.*, 2017, **53**, 12918; (c) J. B. Metternich, D. G. Artiukhin, M. C. Holland, M. von Bremen-Kühne, J. Neugebauer and R. Gilmour, *J. Org. Chem.*, 2017, **82**, 9955; (d) J. Lu, B. Pattengale, Q. Liu, S. Yang, W. Shi, S. Li, J. Huang and J. Zhang, *J. Am. Chem. Soc.*, 2018, **140**, 13719.
- M. Garreau, F. Le Vaillant and J. Waser, *Angew. Chem., Int. Ed.*, 2019, **58**, 8182.
- S. Mukherjee, B. Maji, A. Tlahuext-Aca and F. Glorius, *J. Am. Chem. Soc.*, 2016, **138**, 16200.

